Measurements of the $^{169}\text{Tm}(n,2n)^{168}\text{Tm}$ cross section from threshold to 15 MeV

J. Soter,* M. Bhike, S. W. Finch, Krishichayan, and W. Tornow[†]

Department of Physics, Duke University Durham, North Carolina 27708, USA

and Triangle Universities Nuclear Laboratory, Durham, North Carolina 27708, USA

(Received 11 October 2017; revised manuscript received 21 November 2017; published 27 December 2017)

Measurements of the 169 Tm $(n,2n)^{168}$ Tm cross section have been performed via the activation technique at 13 energies between 8.5 and 15.0 MeV. The purpose of this comprehensive data set is to provide an alternative diagnostic tool for obtaining subtle information on the neutron energy distribution produced in inertial confinement deuterium-tritium fusion experiments at the National Ignition Facility (NIF) at Lawrence Livermore National Laboratory. The 169 Tm $(n,2n)^{168}$ Tm reaction not only provides the primary 14-MeV neutron fluence, but also the important down-scattered neutron fluence, the latter providing information on the density achieved in the deuterium-tritium plasma during a laser shot.

DOI: 10.1103/PhysRevC.96.064619

I. INTRODUCTION

For practical reasons, monoisotopic chemical elements play an important role in applied nuclear physics. The rareearth-metal element thulium with Z = 63 and A = 169 is no exception. Its (n,2n) Q value of -8.1 MeV and the decay radiation of the daughter nucleus 168Tm make thulium a convenient diagnostic tool for measuring the neutron fluence in laser shots at the National Ignition Facility (NIF), located at Lawrence Livermore National Laboratory. There deuteriumtritium (DT) loaded capsules are bombarded with powerful lasers with the goal of achieving ignition. Until now this goal has not been met, and efforts are under way to understand the complicated physics governing the plasma-laser interaction. Because of the high instantaneous neutron flux from the $d + T \rightarrow n + \alpha$ reaction, traditional neutron time-of-flight techniques employing even the fastest plastic-scintillatorbased neutron detectors and associated photomultiplier tubes reach the limits of their applicability. Therefore, passive methods for neutron fluence determination are an important alternative [1]. The 169 Tm $(n,2n)^{168}$ Tm reaction probes the primary and down-scattered neutron energy spectrum from the $d + T \rightarrow n + \alpha$ reaction with maximum energy of 14.7 MeV. Because of the high deuterium, tritium, and neutron density within the DT plasma, there is a finite probability for secondary reactions, i.e., elastic and inelastic neutron scattering off deuterons and tritons, resulting in lower energy, so-called down-scattered neutrons [2]. Valuable information on the plasma density could be obtained if the $^{169}\text{Tm}(n,2n)^{168}\text{Tm}$ cross section is accurately known. Recent work [3,4] has focused on the $^{169}\text{Tm}(n,3n)^{167}\text{Tm}$ reaction with a Q value of -15.0 MeV. This reaction probes the reaction-in-flight (RIF) neutrons, which could have energies up to 30 MeV [5]. Again, their fluence is a measure of the DT plasma density. Considerably stronger conclusions can be drawn, however, if both down-scattered and RIF neutron fluence can be measured simultaneously in the same laser shot. This is the main motivation for the present $^{169}\text{Tm}(n,2n)^{168}\text{Tm}$ cross-sectional measurements.

The $^{169}\text{Tm}(n,2n)^{168}\text{Tm}$ cross section has been heavily investigated in the 14-MeV energy range. In contrast, data below this energy are scarce. Figure 1 shows the experimental information available for the $^{169}\text{Tm}(n,2n)^{168}\text{Tm}$ cross section from threshold up to 12.5 MeV in comparison to the commonly used nuclear data evaluations JEFF-3.2, JENDL-4.0 [6], IRDF-2002, and ENDF/B-VII.1 [7]. Focusing on this energy range, which is important to probe down-scattered neutrons at NIF, and ignoring the very early (1960) data of Tewes et al. [8], we note that in addition to the comprehensive data set of Frehaut et al. [9] there exist only two data points from Bayhurst et al. [10]. In contrast to the vast majority of (n,2n) data reported in the literature, which are based on the well-known activation technique, Frehaut et al. detected the outgoing neutrons directly, using a sophisticated detector and analysis procedure, which have not been duplicated by any other group. The lack of sufficient (n,2n) data below 12 MeV was one of the main reasons for the present study.

II. EXPERIMENTAL SETUP AND PROCEDURE

The experimental setup, data collection, and data analysis procedures are identical to those of Ref. [11]. In short, we used the neutron activation technique to measure the 169 Tm $(n,2n)^{168}$ Tm cross section. The 2 H $(d,n)^{3}$ H reaction was employed to produce mono-energetic neutrons in 0.5-MeV energy steps between 8.5 and 14 MeV. The 197 Au $(n,2n)^{196}$ Au reaction served as neutron fluence monitor. In order to extend the energy range to higher energies, the ${}^{3}\mathrm{H}(d,n){}^{4}\mathrm{H}$ reaction was used at 14.8 MeV. At such a high energy, the 169 Tm $(n,2n)^{168}$ Tm and 197 Au $(n,2n)^{196}$ Au reactions would be sensitive to so-called breakup neutrons from the ${}^{2}\mathrm{H}(d,n){}^{3}\mathrm{He}$ reaction. In order to avoid making the associated corrections, the ${}^{3}\text{H}(d,n)^{4}\text{He}$ reaction with its large Q value of 17.59 MeV was employed. The TUNL tandem accelerator facility [12] provided and accelerated the deuteron beams. The thulium samples consisted of 11.1-mm-diameter disks of 0.1 mm thickness. They were positioned at a distance of 2.5 cm from the end of the deuterium gas cell described in Ref. [13], or from

^{*}Present address: Drew University.

[†]tornow@tunl.duke.edu

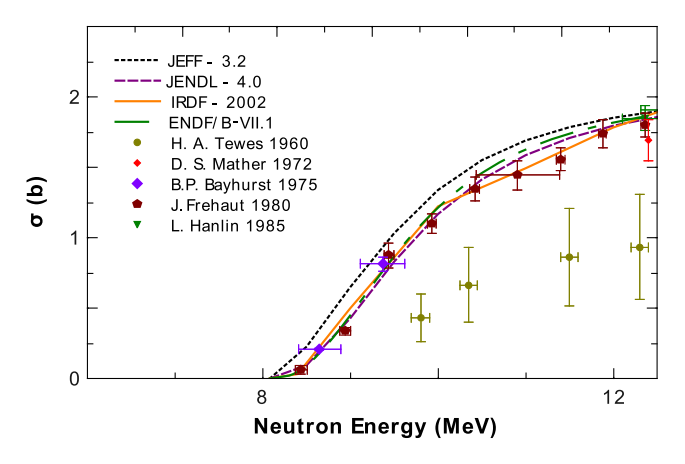


FIG. 1. Available literature data and evaluations for the $^{169}\mathrm{Tm}(n,2n)^{168}\mathrm{Tm}$ cross section from threshold to 12.5 MeV. The horizontal error bars illustrate the spread of neutron energies used in the experiment.

the tritiated titanium target foil described in Ref. [14]. The thulium disks were sandwiched between two monitor foils of 197 Au of the same diameter as the thulium disks and 0.025 mm thick. Irradiation times varied between 2 and 8 h, depending on neutron source reaction and energy. After irradiation, the thulium and monitor foils were γ -ray counted in TUNL's Low-Background Counting Facility using 25%, 55%, or 60% relative efficiency (with respect to a 3" × 3" NaI detector) high-purity germanium (HPGe) detectors. The samples were positioned at a distance of 5.0 cm from the front face of the detectors. The γ -ray energies of interest and other relevant information are given in Table I for 169 Tm and 197 Au. The 168 Tm nucleus undergoes electron capture to form 168 Er.

III. DATA ANALYSIS

Using the Canberra Multiport II data-acquisition system with associated GENIE software, the activity of the samples was followed until the initial activity was determined to sufficient accuracy. Figure 2 shows a γ -ray energy spectrum obtained at $E_n=11.91$ MeV. For comparison, a background spectrum measured before irradiation is also shown, indicating a potential interference problem with an environmental background line in the case of the 184.3-keV transition in 168 Er. The well-known 355.73-keV neutron monitor transition in 196 Au was background free. Parts of the relevant level scheme of 168 Er are displayed in Fig. 3. As can be seen, 168 Er has strong γ -ray transitions. Figure 4 shows typical decay curves

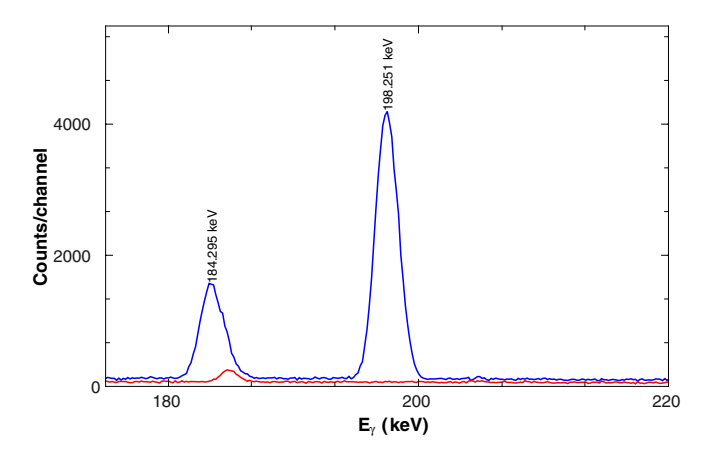


FIG. 2. γ -ray energy spectra, expanded around the 200-keV region, obtained with a HPGe detector after 5 h of irradiation with a 11.91 ± 0.11 MeV neutron beam. The activated sample spectra is shown in blue and the background spectrum, measured before irradiation, is shown in red.

at selected incident neutron energies for 168 Tm and 196 Au. Within uncertainties, the measured decay half-life times $T_{1/2}$ agree with the literature values.

The photo-peak efficiency of the HPGe detectors used in the present work was determined with calibrated test sources. Typical efficiency data and associated fit results are shown in Fig. 5.

In order to obtain the cross-sectional values of interest, the activation formula [16] is first used to obtain the neutron flux ϕ_n from the measured activity of ¹⁹⁶Au,

$$\phi_n = \frac{A\lambda}{N\sigma\epsilon I_{\gamma}(1 - e^{-\lambda t_i})e^{-\lambda t_d}(1 - e^{-\lambda t_m})},$$
 (1)

where the induced activity A is the total yield in the photopeak, N is the total number of target nuclei, ϵ is the photopeak efficiency for the γ -ray energy of interest, I_{γ} is its intensity, t_i is the irradiation time, t_d is the decay time between the end of irradiation and the begin of off-line counting, and t_m is the measuring time. The cross-sectional values, σ , for the 197 Au $(n,2n)^{196}$ Au reaction were taken from Ref. [17].

Next, the activation formula is employed once more, this time with the induced activity of the 169 Tm foils and ϕ_n obtained as described above, to determine the 169 Tm $(n,2n)^{168}$ Tm cross section of interest:

$$\sigma = \frac{A\lambda}{N\phi_n \epsilon I_{\nu} (1 - e^{-\lambda t_i}) e^{-\lambda t_d} (1 - e^{-\lambda t_m})},$$
 (2)

where the notations follow those of Eq. (1).

TABLE I. Relevant data for the reactions of interest in the present work.

Reaction	Threshold [MeV]	Half-life	Isotopic abundance	$ ext{E}_{\gamma} ext{ [keV]}$	$egin{array}{c} egin{array}{c} \egin{array}{c} \egin{array}{c} \egin{array}{c} \egin{array}$
169 Tm $(n,2n)^{168}$ Tm	8.082	93.1 (2) d	100	184.295 (2)	18.15 (16)
				198.251 (2)	54.49 (16)
				447.515 (3)	23.98 (11)
				815.989 (5)	50.95 (16)
$^{197}\mathrm{Au}(n,2n)^{196}\mathrm{Au}$	8.114	6.1669 (6) d	100	355.73 (5)	87

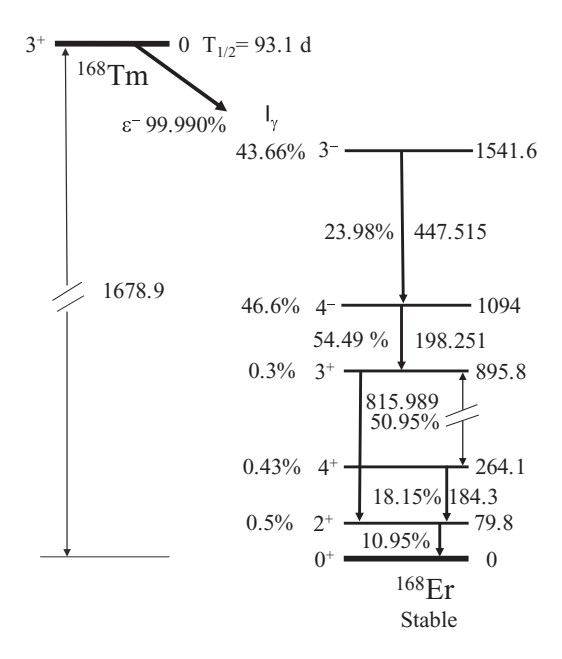


FIG. 3. Partial level scheme for decay of ¹⁶⁸Tm, showing all transitions measured in the present work. All energies are given in keV. Data taken from Ref. [15].

We restricted ourselves to the strongest (198.251-keV) transition. As pointed out already, the 184.295-keV transition is affected by a background line. The 815.989-keV γ ray has a similar intensity as the 198.251-keV transition, but its detection efficiency is more than a factor of three lower than that of the 198.251-keV transition. The transitions at 447.515 and 815.989 keV also required larger summing corrections than the 198.251-keV γ -ray line. The coincidence summing corrections for the 198.251-keV transition varied between 1.5% and 4.5%, depending on the HPGe detector used to record the induced activity. The summing correction was confirmed by taking data with the same sample at 5 and 15 cm from the detector face. This was easily achievable given the long-lived activity of ¹⁶⁸Tm. For measurements made at a 15-cm distance, summing effects were found to be negligible. When determining final cross-sectional values, the summing effects were corrected for accordingly.

It should also be noted that the 447.515-keV transition yield consistently gave smaller cross-sectional values than the 198.251- or 815.989-keV transitions, indicating a problem with the published I_{γ} value. With the sample positioned 15 cm from the detector, the intensity ratio of the two strongest γ -ray transitions in $^{168}\rm{Er}$, 198.251 and 815.989 keV, was consistent with the literature value [15], within our experimental uncertainties. The intensity ratio of the 198.521-keV γ ray and the third strongest transition at 447.515-keV, however, was measured to be 2.60 \pm 0.08, in contrast to the literature intensity ratio of 2.27 \pm 0.02.

IV. RESULTS

Results for the $^{169}\text{Tm}(n,2n)^{168}\text{Tm}$ reaction cross section are shown in Fig. 6 in comparison to the existing data and evaluations. Our data confirm those of Frehaut *et al.*, the only

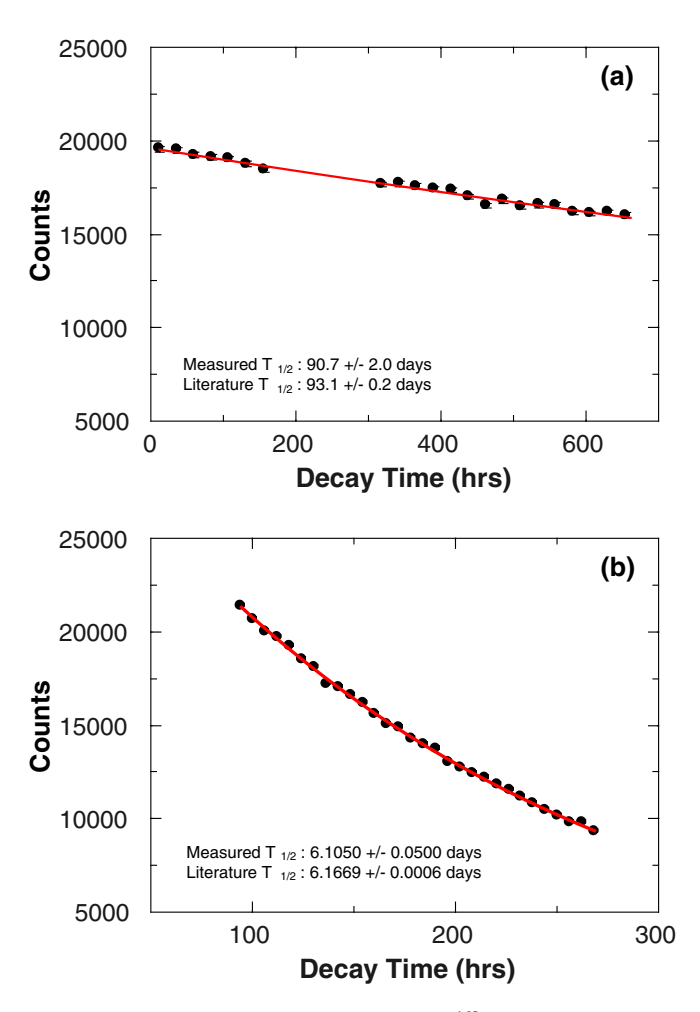


FIG. 4. Measured decay curves of the (a) ¹⁶⁸Tm 198-keV activity after irradiation with 12.41-MeV neutrons and (b) ¹⁹⁶Au 355-keV activity after irradiation with 12.90-MeV neutrons. The data are fit to an exponential decay (red curves).

previously available comprehensive data set below 12-MeV neutron energy, as well as the two data points of Bayhurst *et al.* With our improved accuracy, the $^{169}\text{Tm}(n,2n)^{168}\text{Tm}$

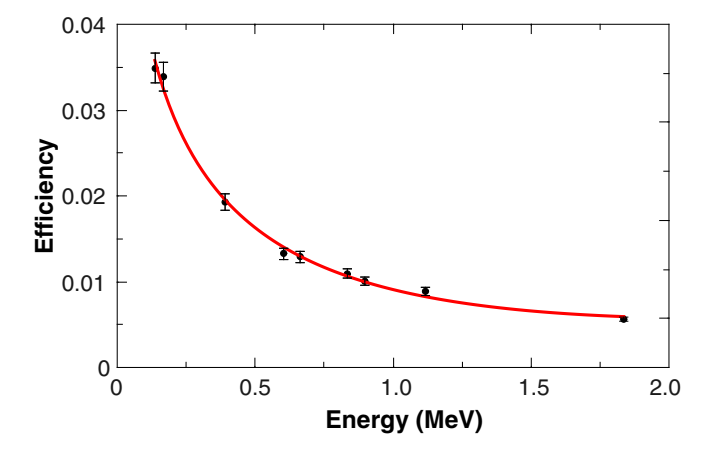


FIG. 5. Measured efficiency data and fit (red curve) using a mixed γ -ray source positioned 5 cm away from the face of a 55% relative efficiency HPGe detector. The efficiency was fit to a function of the form $\sum_{i=0}^{3} \epsilon_i \ln(E)^i$, where ϵ_i are free parameters.

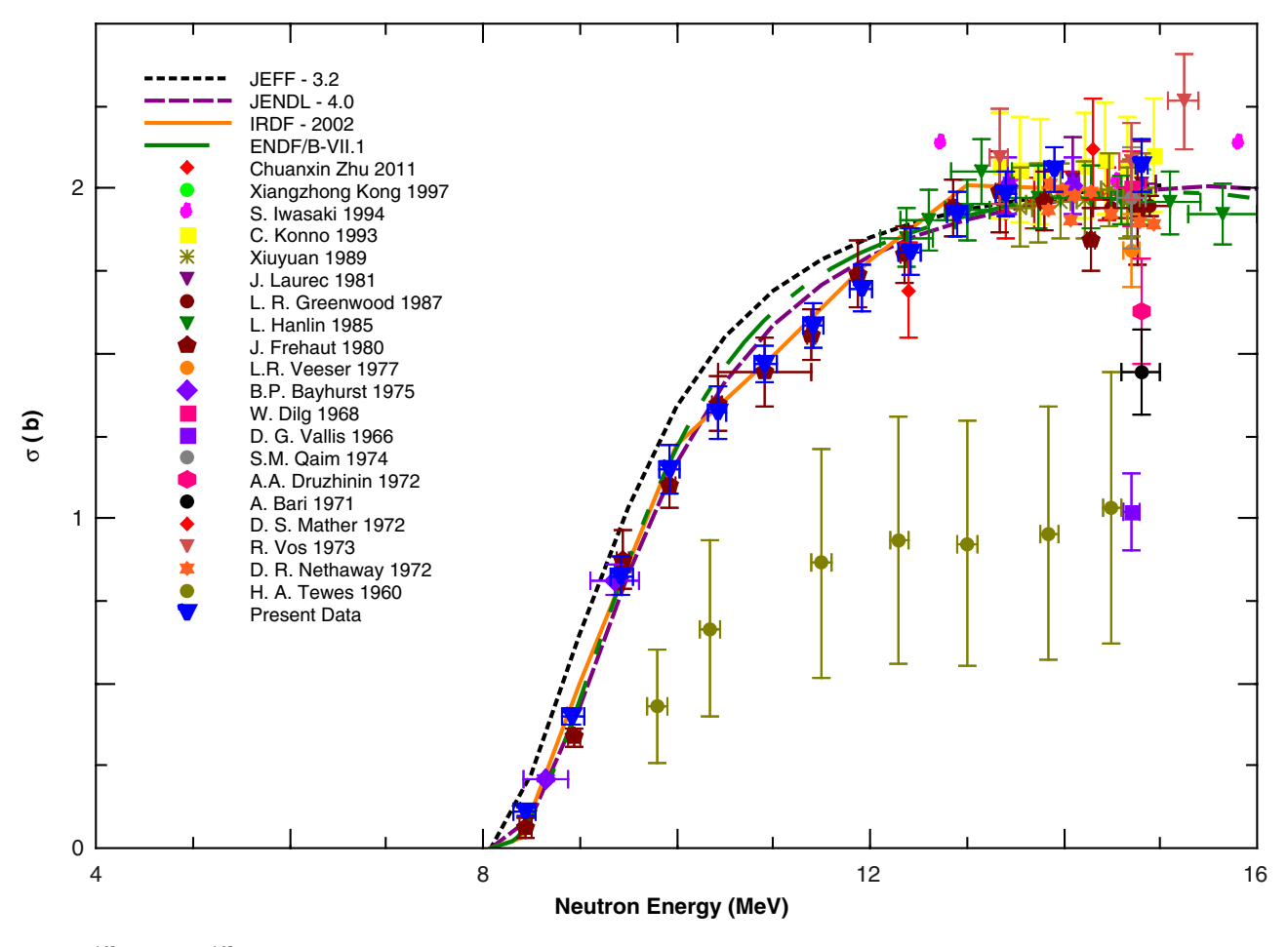


FIG. 6. 169 Tm $(n,2n)^{168}$ Tm cross-sectional data in comparison to evaluations and previous data. The horizontal error bars indicate the neutron energy spread for the present experiment.

cross section is now very well determined in this energy range above the reaction threshold. At higher energies, our data agree very well with the average of the existing data in the 13- to 15-MeV energy region. The existing evaluations all meet at 14 MeV. The largest difference between them can be seen in the 11-MeV energy region. Here the IRDF-2002 evaluation follows the trend of the experimental data, while the JENDL-4.0 and ENDF/B-VII.1 evaluations are somewhat higher in the 11- to 12-MeV energy range. There is hardly any difference between the JENDL-4.0 and ENDF/B-VII.1 evaluations. The JEFF-3.2 evaluation overestimates all data below 12 MeV.

An excellent agreement was found using the TALYS-based evaluated nuclear data library (TENDL-2015) [18]. TENDL uses the output of the TALYS nuclear model calculation and is shown in Fig. 7, along with the present data. The largest deviation between our data and TALYS comes near threshold at the 8.43-MeV data point. Otherwise, the excellent agreement indicates that cross-sectional data are well modeled by TALYS and the default parameters are well chosen in this mass range.

Our results are presented in numerical form in Table II. The first column gives the mean neutron energy. The second column provides the monitor reaction cross-sectional

data used to obtain the results given in column 3 for the $^{169}\text{Tm}(n,2n)^{168}\text{Tm}$ cross section. The uncertainty budget is summarized in Table III.

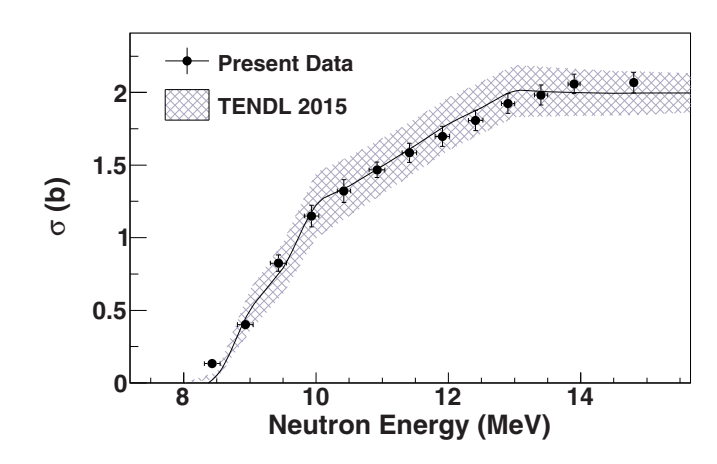


FIG. 7. The present data compared with the TENDL-2015 output of the TALYS calculation. The calculation with the default parameters is shown by the solid black curve, with the shaded region showing the range of results achieved by varying the parameters.

TABLE II. 169 Tm $(n,2n)^{168}$ Tm reaction: neutron energy and associated energy spread, 197 Au $(n,2n)^{196}$ Au reaction cross-sectional data used for determining the neutron fluence, and cross-sectional results obtained for the 169 Tm $(n,2n)^{168}$ Tm reaction.

Monitor σ [mb]	169 Tm $(n,2n)^{168}$ Tm σ [mb]
77.85 ± 6.34 304.9 ± 11.8 651.5 ± 21.8 978.8 ± 29.7 1222.1 ± 35.8 1420.8 ± 39.2 1577.6 ± 41.9 1713.3 ± 43.6 1834.6 ± 43.9 1944.1 ± 41.7 2043.7 ± 34.2 $2119.9 + 25.3$	133.4 ± 12.4 401.3 ± 23.9 825.0 ± 56.6 1149.3 ± 74.4 1321.9 ± 78.5 1467.1 ± 53.6 1584.3 ± 66.0 1697.4 ± 69.3 1807.6 ± 69.7 1923.6 ± 68.4 1982.4 ± 68.6 2058.4 ± 67.1
	$\sigma \text{ [mb]}$ 77.85 ± 6.34 304.9 ± 11.8 651.5 ± 21.8 978.8 ± 29.7 1222.1 ± 35.8 1420.8 ± 39.2 1577.6 ± 41.9 1713.3 ± 43.6 1834.6 ± 43.9 1944.1 ± 41.7

V. CONCLUSION

This work presents an accurate and comprehensive crosssectional data set for the $^{169}\text{Tm}(n,2n)^{168}\text{Tm}$ reaction from threshold to 15 MeV. The present data favor the IRDF-2002, ENDF/B-VII.1, and JENDL-4.0 evaluations over those of JEFF-3.2. The results of our measurements provide an improved basis for determining the down-scattered neutron fluence component obtained in laser shots on DT capsules

[1] J. A. Frenje, R. Bionta, E. J. Bond, J. A. Caggiano, D. T. Casey, C. Cerjan, J. Edwards, M. Eckart, D. N. Fittinghoff, S. Friedrich et al., Nucl. Fusion 53, 043014 (2013).

TABLE III. Uncertainty budget.

Uncertainty	Tm [%]	Monitors [%]
Counting statistics	0.1–1.6	0.03-0.60
Reference cross section		1.1-8.1
Detector efficiency	0.81 - 7.77	2.4-4.8
Half-life	0.21	0.01
γ -ray intensity		0.29
Coincidence summing	3–5	1–3
Source geometry and		
Self-absorption of γ rays	< 0.5	< 0.5
Irradiation time	< 0.5	< 0.5
Decay time	< 0.5	< 0.5
Counting time	< 0.5	< 0.5
Neutron flux fluctuation	< 0.5	< 0.5

at NIF. This diagnostic tool is expected to give valuable information on the density of the inertial confinement fusion plasma.

ACKNOWLEDGMENTS

This work was supported in part by the National Nuclear Security Administration under Grant No. DE-NA0002936 and the U.S. Department of Energy, Office of Nuclear Physics, under Grant No. DE-FG02-97ER41033. J. Soter acknowledges support from the NSF Research Experience for Undergraduate (REU) students program, under Grant No. NSF-PHY-1461204.

- [9] J. Frehaut, A. Bertin, R. Bois, and J. Jary, in *Symposium on Neutron Cross Sections from 10–50 MeV*, edited by M. Bhat and S. Pearlstein (National Technical Information Service, Springfield, Va., 1980).
- [10] B. P. Bayhurst, J. S. Gilmore, R. J. Prestwood, J. B. Wilhelmy, N. Jarmie, B. H. Erkkila, and R. A. Hardekopf, Phys. Rev. C 12, 451 (1975).
- [11] M. Bhike, B. Fallin, M. E. Gooden, N. Ludin, and W. Tornow, Phys. Rev. C 91, 011601 (2015).
- [12] [http://www.tunl.duke.edu/web.tunl.2011a.tandem.php].
- [13] C. Bhatia, S. W. Finch, M. E. Gooden, and W. Tornow, Phys. Rev. C **86**, 041602(R) (2012).
- [14] C. Bhatia, S. W. Finch, M. E. Gooden, and W. Tornow, Phys. Rev. C 87, 011601(R) (2013).
- [15] [http://www.nndc.bnl.gov/chart/decaysearchdirect.jsp? nuc=168TM1.
- [16] M. Bhike and W. Tornow, Phys. Rev. C 89, 031602(R) (2014).
- [17] K. I. Zolotarev, Re-evaluation of microscopic and integral cross-section data for important dosimetry reactions, Tech. Rep. INDC(NDS)-0526 (International Atomic Energy Agency, 2008).
- [18] A. Koning and D. Rochman, Nucl. Data Sheets 113, 2841 (2012).

^[2] P. A. Bradley, G. P. Grim, A. C. Hayes, G. Jungman, R. S. Rundberg, J. B. Wilhelmy, G. M. Hale, and R. C. Korzekwa, Phys. Rev. C 86, 014617 (2012).

^[3] B. Champine, M. E. Gooden, Krishichayan, E. B. Norman, N. D. Scielzo, M. A. Stoyer, K. J. Thomas, A. P. Tonchev, W. Tornow, and B. S. Wang, Phys. Rev. C 93, 014611 (2016).

^[4] M. E. Gooden, T. A. Bredeweg, B. Champine, D. C. Combs, S. Finch, A. Hayes-Sterbenz, E. Henry, Krishichayan, R. Rundberg, W. Tornow, J. Wilhelmy, and C. Yeamans, Phys. Rev. C 96, 024622 (2017).

^[5] J. Lindl, O. Landen, J. Edwards, and E. Moses, Phys. Plasmas 21, 020501 (2014).

^[6] K. Shibata, O. Iwamoto, T. Nakagawa, N. Iwamoto, A. Ichihara, S. Kunieda, S. Chiba, K. Furutaka, N. Otuka, T. Ohasawa *et al.*, J. Nucl. Sci. Technol. 48, 1 (2011).

^[7] M. B. Chadwick, M. Herman, P. Obložinský, M. E. Dunn, Y. Danon, A. C. Kahler, D. L. Smith, B. Pritychenko, G. Arbanas, R. Arcilla *et al.*, Nucl. Data Sheets 112, 2887 (2011).

^{[8] [}https://www.nndc.bnl.gov/exfor/servlet/X4sGetSubent?reqx= 55938&subID=11504014].